AMERICAN SOCIETY FOR MICROBIOLOGY | Infection and Immunity®

MOLECULAR PATHOGENESIS

Association of Metal Homeostasis and (p)ppGpp Regulation in the Pathophysiology of *Enterococcus faecalis*

C. Colomer-Winter,[a] A. O. Gaca,[b]* J. A. Lemos[a]

Department of Oral Biology, University of Florida College of Dentistry, Gainesville, Florida, USA[a]; Center for Oral Biology and Department of Microbiology and Immunology, University of Rochester Medical Center, Rochester, New York, USA[b]

ABSTRACT In *Enterococcus faecalis*, the regulatory nucleotides pppGpp and ppGpp, collectively, (p)ppGpp, are required for growth in blood, survival within macrophages, and virulence. However, a clear understanding of how (p)ppGpp promotes virulence in *E. faecalis* and other bacterial pathogens is still lacking. In the host, the essential transition metals iron (Fe) and manganese (Mn) are not readily available to invading pathogens because of a host-driven process called nutritional immunity. Considering its central role in adaptation to nutritional stresses, we hypothesized that (p)ppGpp mediates *E. faecalis* virulence through regulation of metal homeostasis. Indeed, supplementation of serum with either Fe or Mn restored growth and survival of the Δ*rel* Δ*relQ* [(p)ppGpp^0] strain to wild-type levels. Using a chemically defined medium, we found that (p)ppGpp accumulates in response to either Fe depletion or Mn depletion and that the (p)ppGpp^0 strain has a strong growth requirement for Mn that is alleviated by Fe supplementation. Although inactivation of the nutrient-sensing regulator *codY* restored some phenotypes of the (p)ppGpp^0 strain, transcriptional analysis showed that the (p)ppGpp/CodY network does not promote transcription of known metal transporters. Interestingly, physiologic and enzymatic investigations suggest that the (p)ppGpp^0 strain requires higher levels of Mn in order to cope with high levels of endogenously produced reactive oxygen species (ROS). Because (p)ppGpp mediates antibiotic persistence and virulence in several bacteria, our findings have broad implications and provide new leads for the development of novel therapeutic and preventive strategies against *E. faecalis* and beyond.

KEYWORDS (p)ppGpp, *Enterococcus*, manganese, metal homeostasis, nutritional immunity, oxidative stress

Enterococcus faecalis is a common member of the human gut microbiota but also a leading cause of a number of hospital-acquired infections such as endocarditis and surgical wound and urinary tract infections (1). The association of this opportunistic pathogen with disease relies on its exceptional resilience, which allows it to prevail in the unfavorable hospital setting while providing a competitive advantage over other bacteria during both infection and treatment.

Among the most prominent regulators involved in bacterial adaptation to stress are the nucleotide second messengers guanosine tetraphosphate (ppGpp) and guanosine pentaphosphate (pppGpp), collectively, (p)ppGpp, best known as the effectors of the stringent response (SR) (2). While initially discovered to accumulate in response to amino acid starvation, (p)ppGpp has also been shown to accumulate in response to restrictions in carbon, fatty acids, and iron, as well as in response to other nonnutritional stresses (3). During the SR, (p)ppGpp accumulation triggers transcriptional alterations that lead to general repression of rapid growth and simultaneous activation of stress survival, nutrient uptake, and biosynthesis pathways. In addition to its involvement in transcriptional control, (p)ppGpp allosterically inhibits the activity of several

Received 10 April 2017 **Accepted** 2 May 2017

Accepted manuscript posted online 8 May 2017

Citation Colomer-Winter C, Gaca AO, Lemos JA. 2017. Association of metal homeostasis and (p)ppGpp regulation in the pathophysiology of *Enterococcus faecalis*. Infect Immun 85:e00260-17. https://doi.org/10.1128/IAI.00260-17.

Editor Shelley M. Payne, University of Texas at Austin

Address correspondence to J. A. Lemos, jlemos@dental.ufl.edu.

* Present address: A. O. Gaca, Massachusetts Eye and Ear Infirmary, Harvard Medical School, Boston, Massachusetts, USA.

enzymes, including DNA primase, translation factors, and enzymes involved in GTP biosynthesis (3, 4). Moreover, modest increases in (p)ppGpp levels, below those required to activate the SR, have been shown to contribute to restoration of cellular homeostasis under mildly stressful conditions (3).

Because the success of pathogens is directly linked to their ability to adapt to host-derived stresses, it is not surprising that (p)ppGpp regulation is tightly associated with virulence (5). Previous characterization of *E. faecalis* strains defective in (p)ppGpp production revealed that a complete lack of (p)ppGpp [(p)ppGpp^0 strain] led to attenuated virulence in two invertebrate animal models and in a rabbit subdermal abscess model (6–8). In addition, the (p)ppGpp^0 strain displayed impaired survival within macrophages as well as a growth and survival defect in whole blood and serum *ex vivo* (7, 8). The importance of (p)ppGpp to *E. faecalis* pathogenesis is further underscored by a transcriptome analysis of cells isolated from rabbit abscesses. In this study, a transcriptional expression pattern reminiscent of the SR was identified, suggesting that (p)ppGpp accumulates during the early stages of infection, possibly mediating adaptation to the host environment (8). Considering the central role of (p)ppGpp in adaptation to nutritional stresses and the impaired growth and survival of the (p)ppGpp^0 strain under *ex vivo* and *in vivo* conditions, we hypothesized that (p)ppGpp might contribute to the virulence of *E. faecalis* by mediating adaptation to nutrient limitation within the host.

The elements iron (Fe) and manganese (Mn) are essential micronutrients for virtually all forms of life (9). In bacteria, Fe acts as the cofactor for enzymes involved in energy generation and DNA, amino acid, and vitamin biosynthesis (10, 11). Despite being an essential micronutrient, intracellular Fe levels must be tightly controlled to avoid the deleterious effects of hydroxyl radicals that are generated via the Fenton reaction (12). While Mn is also involved in DNA synthesis and in a number of other metabolic pathways, the role of this transition metal has been largely attributed to oxidative stress tolerance because it is not subjected to Fenton chemistry, it serves as the cofactor of Mn-dependent superoxide dismutases (MnSOD), and it may substitute for Fe as the cofactor in a variety of Fe-binding enzymes (9, 13–16). This is especially true for lactic acid bacteria such as *E. faecalis*, since members of this group are thought to require higher intracellular amounts of Mn to protect themselves from metabolically generated reactive oxygen species (ROS) (14). Notably, lactic acid bacteria have been shown to accumulate millimolar concentrations of intracellular Mn during ROS stress (14, 15).

Efficient acquisition of Fe and Mn by bacterial pathogens has been shown to contribute to their success during infection (9, 16, 17). In the host, Fe and Mn are mostly found in tight association with hemoproteins such as hemoglobin. In addition, other metalloproteins such as transferrin, ferritin, and calprotectin rapidly remove free metals from blood, tissues, and the intracellular milieu, thereby limiting metal availability to invading bacteria through an active process known as nutritional immunity (11, 16). As a result, the nutritional immunity contributes to clearance of invading microbes in two distinct but additive ways: (i) by inhibiting growth of pathogens during systemic infection due to metabolic failure and (ii) by hampering survival of bacteria exposed to the oxidative burst of macrophages and neutrophils (11, 16). To survive the host-imposed metal limitation, bacteria typically express high-affinity metal transporters and siderophores that scavenge these micronutrients from the host, ultimately allowing bacteria to maintain metal homeostasis (11, 16).

Since Fe and Mn are limiting nutrients during infection, we hypothesized that (p)ppGpp contributes to the virulence of *E. faecalis* through regulation of metal homeostasis. In support of this hypothesis, we found that addition of Fe or Mn to serum restored growth and survival of the (p)ppGpp^0 strain to wild-type levels. Using controlled laboratory conditions, we showed that the (p)ppGpp^0 strain has a strong growth requirement for Mn that is partially compensated by Fe supplementation. However, (p)ppGpp did not mediate adaptation to Mn restriction through activation of Mn transporters. Instead, we found that the strong Mn requirement of the (p)ppGpp^0 strain is, in part, due to endogenous ROS generated by its metabolic dysregulation (18). To

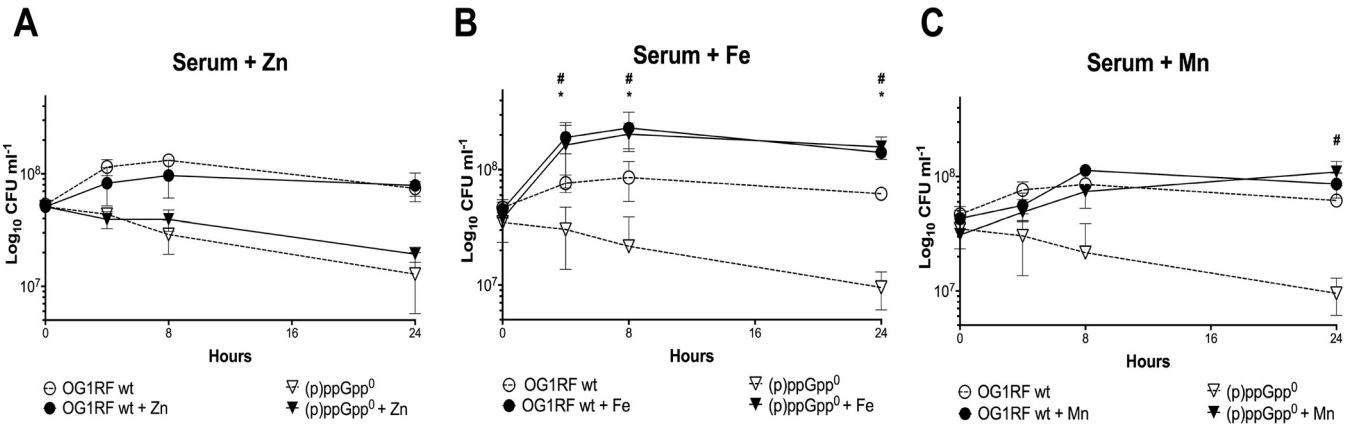

FIG 1 Growth behavior of *E. faecalis* in horse serum. Data represent growth of *E. faecalis* wild-type (OG1RF) and (p)ppGpp^0 strains in horse serum with (solid) or without (dashed) metal supplementation. (A) 1 mM $ZnSO_4$. (B) 1 mM $FeSO_4$. (C) 1 mM $MnSO_4$. Aliquots taken at selected time points were serially diluted and plated on TSA plates for CFU enumeration. The graphs show averages and standard deviations of results from three independent experiments. Significant differences in growth of the wild-type (*) and (p)ppGpp^0 (#) strains compared to growth in metal-poor serum were assessed for each time point ($P < 0.05$).

our knowledge, this is the first report directly linking (p)ppGpp-related phenotypes to metal homeostasis. Collectively, our findings reveal that (p)ppGpp, through maintenance of a balanced metabolism, allows the multidrug-resistant pathogen *E. faecalis* to grow and survive in metal-restricted environments. Given the prominent role of (p)ppGpp in bacterial pathogenesis, this report provides leads for the development of new antimicrobial therapies.

RESULTS

Metal supplementation restores growth and survival of the (p)ppGpp^0 strain in serum. As previously mentioned, free Fe and Mn are kept at very low (~10 nM) levels in the bloodstream and upregulation of metal scavenging systems is an integral part of the adaptive response of bacteria during invasive infections (11, 16, 19). Specifically, transcriptomic and proteomic analysis demonstrated that *E. faecalis* strongly induces several high-affinity Fe, Mn, and Zn transporters in blood and urine, suggesting that acquisition of these trace elements is important for growth and persistence of *E. faecalis* in the host environment (19–21). To test if the growth and survival defects of the *E. faecalis* Δ*rel* Δ*relQ* [(p)ppGpp^0] strain in blood (or serum) are due to metal starvation, growth and survival of the parent (OG1RF) and (p)ppGpp^0 strains were monitored in plain horse serum (HS) or HS supplemented with 1 mM $FeSO_4$, 1 mM $MnSO_4$, or 1 mM $ZnSO_4$. Zn is a transition metal essential for protein structure and function that is also withheld from pathogens during systemic infections and was therefore included in our panel of metal cofactors. Consistent with earlier results determined using human serum (8), the Δ*rel* Δ*relQ* strain was unable to grow and survive for extended periods in HS compared to the wild-type strain. While Zn supplementation did not affect growth or survival of the (p)ppGpp^0 strain (Fig. 1A), addition of either Fe (Fig. 1B) or Mn (Fig. 1C) restored growth of the mutant strain to wild-type levels. Notably, Fe supplementation significantly increased final growth yields of both strains in a (p)ppGpp-independent manner.

Lack of (p)ppGpp results in a strong growth requirement for Mn. To investigate the linkage of (p)ppGpp and metal homeostasis in a more controlled fashion, ruling out additional growth-limiting factors present in serum, growth of the OG1RF and Δ*rel* Δ*relQ* strains was monitored in the chemically defined FMC medium depleted for Mn or Fe or both. The depletion of Fe or Mn from ~4 to ~6 μg ml^{-1} in complete FMC medium to below the detection limit (<5 ng ml^{-1}) in the different formulations of metal-depleted FMC was confirmed via inductively coupled plasma-optical emission spectrometry (ICP-OES) (Fig. 2A). We also determined that the Zn concentration in all medium preparations was ~70 ng ml^{-1}. Considering that Zn is not a component of the FMC recipe, these small amounts of Zn were likely due to trace element contamination

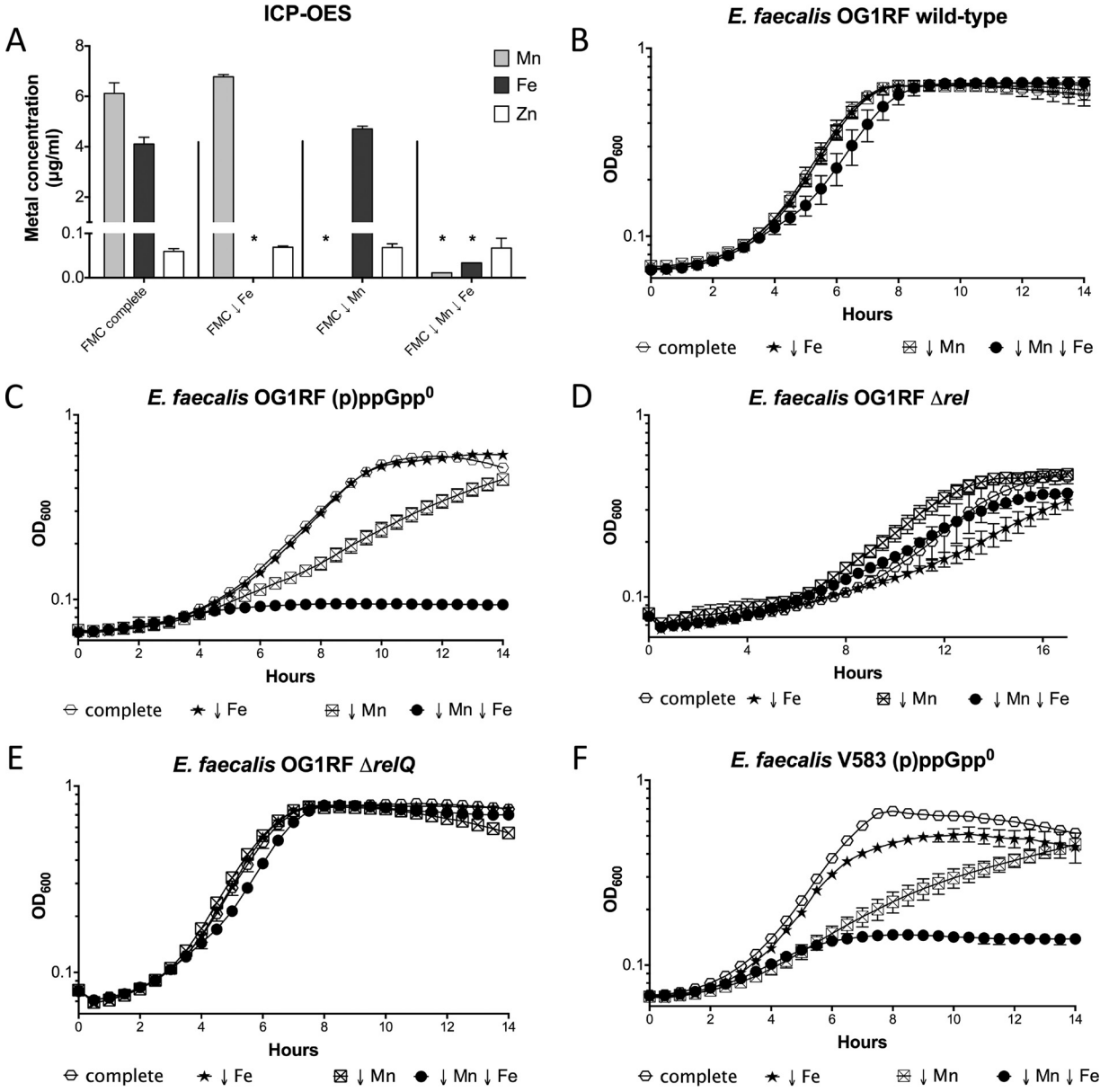

FIG 2 The *E. faecalis* (p)ppGpp^0 strain has a growth requirement for Mn. (A) Total Fe, Mn, and Zn content of the different FMC preparations determined by ICP-OES analysis (*, $P \leq 0.05$). (B to E) Growth of OG1RF and its derivatives in complete and metal-depleted FMC medium. Cells were grown to an OD_{600} of approximately 0.25 in complete FMC medium and diluted 1:100 in FMC medium depleted of Fe or Mn or both. (F) Growth of the *E. faecalis* V583 (p)ppGpp^0 strain in complete or metal-depleted FMC medium. Growth was monitored using a Bioscreen growth reader. The graphs show averages and standard deviations of results from three independent experiments.

of stock reagents. While growth of the parent strain was not affected under conditions of Mn or Fe limitation and was affected only modestly when both metals were depleted (Fig. 2B), the (p)ppGpp^0 strain grew considerably more slowly under Mn-depleted conditions (Fig. 2C). Although Fe depletion did not affect its growth, the (p)ppGpp^0 strain was unable to grow when both metals were depleted. Notably, these phenotypes were restricted to the (p)ppGpp^0 double mutant strain, since growth levels of the Δ*rel* and Δ*relQ* single mutants were unchanged or very modestly altered in metal-depleted media (Fig. 2D and E). Finally, to confirm that these results were not restricted to one strain, we determined the ability of a second *E. faecalis* (p)ppGpp^0 strain, derived from the multidrug-resistant V583 strain, to grow in metal-depleted FMC medium (22). As observed with OG1RF (Fig. 2B), growth of V583 was not affected by single or simultaneous depletion of Mn and Fe (data not shown). However, the growth behavior of the

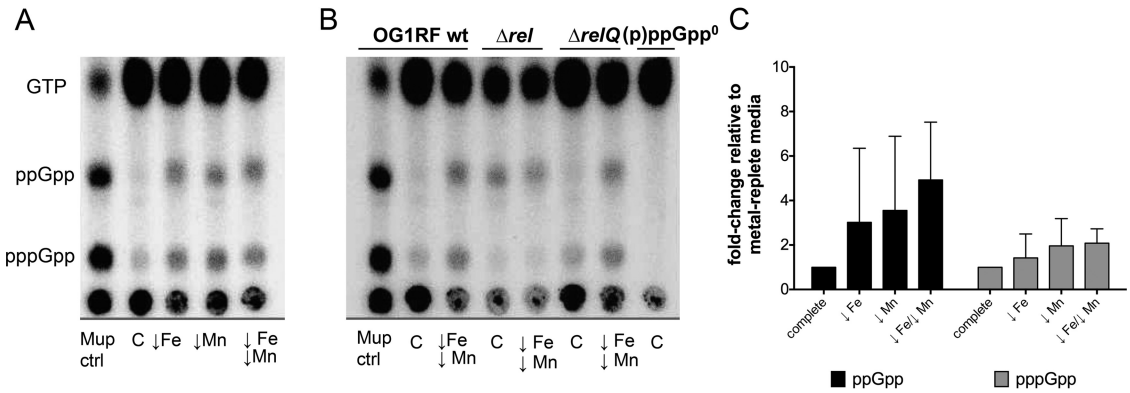

FIG 3 (p)ppGpp accumulates in response to Fe or Mn depletion in a Rel-dependent manner. (A) Mid-exponential-phase OG1RF cultures labeled with [^{32}P]orthophosphate and grown in FMC medium depleted of Fe or Mn or both. As a control, cultures were either grown in complete FMC medium or treated with mupirocin (50 μg ml^{-1}) (Mup ctrl). (B) Mid-exponential-phase cultures of OG1RF, Δ*rel*, Δ*relQ*, and (p)ppGpp^0 (Δ*rel* Δ*relQ*) strains labeled with [^{32}P]orthophosphate were grown in FMC medium depleted of both Fe and Mn. Nucleotide acid extracts were spotted onto PEI-cellulose plates and separated by TLC in 1.25 M KH_2PO_4. wt, wild type. (C) Fold change of ppGpp and pppGpp accumulation in wild-type OG1RF in response to metal depletion relative to metal-replete FMC medium. Relative levels of intensity of (p)ppGpp spots were quantified using the image analysis tool Image J.

V583 (p)ppGpp^0 strain in FMC medium lacking Mn or lacking Mn and Fe was nearly identical to that of the OG1RF (p)ppGpp^0 strain (Fig. 2F).

Fe and Mn limitation leads to *E. faecalis* Rel (Rel_{Ef})-dependent (p)ppGpp accumulation. In *Escherichia coli*, Fe limitation was shown to trigger intracellular (p)ppGpp accumulation (23). Here, we determined the intracellular (p)ppGpp pools in cells grown in Mn- and/or Fe-depleted FMC medium. Depletion of Mn or Fe or both resulted in visibly higher levels of pppGpp and ppGpp pools (Fig. 3A), although the effects were not as strong as the effects caused by isoleucine starvation (mupirocin treatment lane). Even though the results of quantification of (p)ppGpp were not statistically significant due to the inherent variability associated with this assay (Fig. 3C), (p)ppGpp accumulation in response to Fe and/or Mn depletion was consistent across the different experiments.

In *E. faecalis*, (p)ppGpp metabolism is carried out by the bifunctional Rel_{Ef} enzyme and the small alarmone synthetase $RelQ_{Ef}$ (6). To determine which enzyme is responsible for (p)ppGpp accumulation during metal limitation, we also quantified (p)ppGpp pools in the Δrel_{Ef} and Δ$relQ_{Ef}$ strains grown under metal-depleted conditions (Fig. 3B). Even though the Δrel_{Ef} strain displays intrinsically higher (p)ppGpp levels due to the absence of (p)ppGpp hydrolase activity (6, 18), the lack of pppGpp accumulation in this strain indicated that Rel_{Ef} is responsible for (p)ppGpp accumulation in response to metal starvation.

Inactivation of *codY* restores several phenotypes of the (p)ppGpp^0 strain. In *Firmicutes* such as *E. faecalis*, (p)ppGpp controls transcription via two distinct mechanisms: (i) by changing the concentration of the initiating nucleotide of transcription (iNTP) (position +1) and (ii) by modulating the DNA-binding capacity of CodY, a global metabolic regulator of nutrient transport, amino acid biosynthesis, and virulence (3, 4, 24). The ability of nutrient-sensing regulator CodY to bind to DNA and repress target gene expression is strongly enhanced in the presence of branched-chain amino acids (BCAA) and GTP (24). The notable drop in GTP due to (p)ppGpp accumulation alleviates CodY repression, resulting in activation of genes involved in amino acid biosynthesis, nutrient transport, and virulence (24). Inability to synthetize (p)ppGpp maintains elevated GTP levels (18, 25), promoting CodY-mediated repression of these pathways even under stress conditions. As a result, deletion of *codY* in (p)ppGpp^0 background strains of different species restores or ameliorates a variety of (p)ppGpp-related phenotypes, including amino acid auxotrophy and attenuated virulence (24, 25). Here, we used a markerless system to delete the *codY* gene from the parent and (p)ppGpp^0 strains in order to determine if inactivation of *codY* abolishes or alleviates the metal dependence

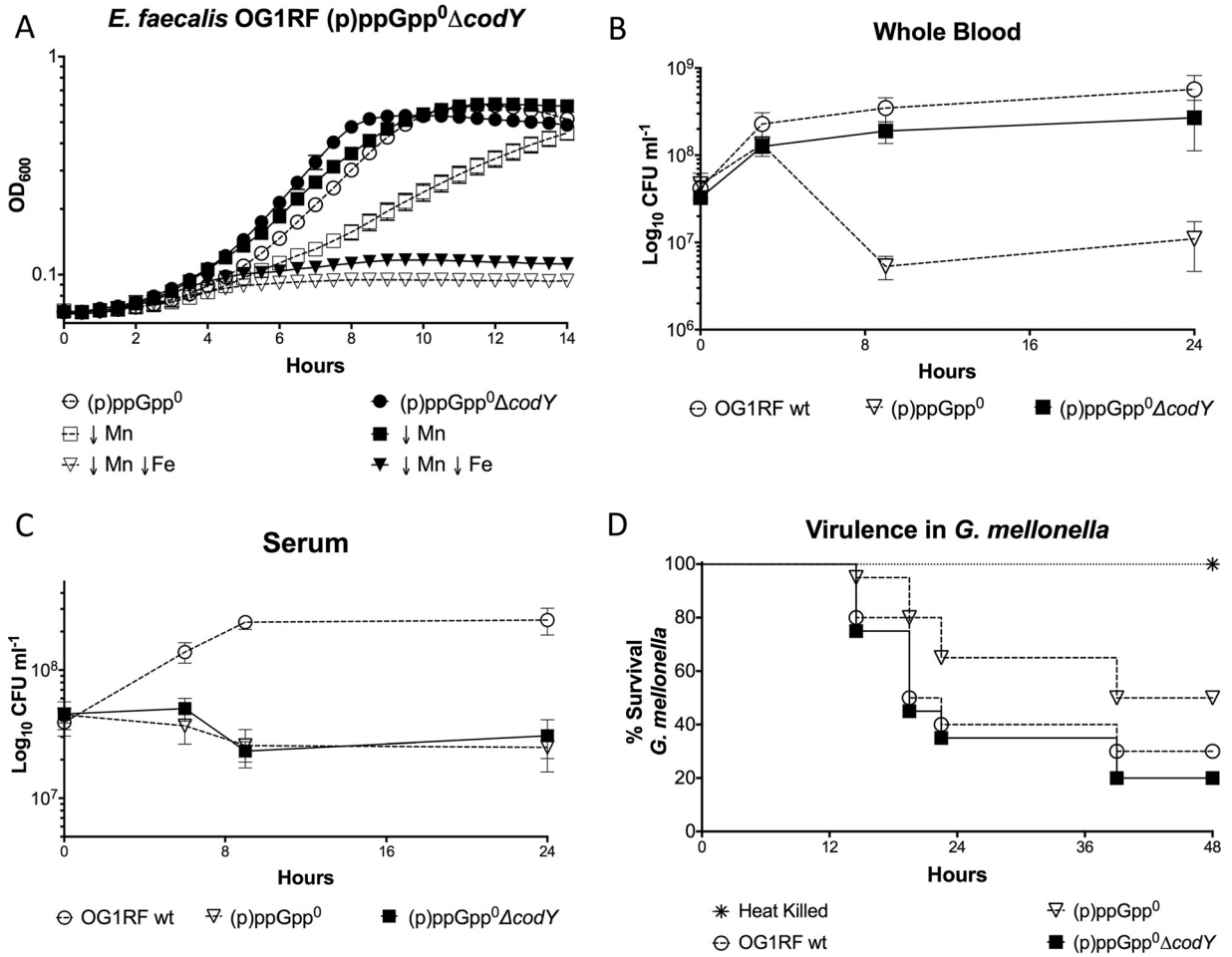

FIG 4 Deletion of *codY* restores several, but not all, (p)ppGpp^0 phenotypes. (A) Growth of *E. faecalis* OG1RF (p)ppGpp^0 (Δ*rel* Δ*relQ*) and Δ*rel* Δ*relQ* Δ*codY* strains in metal-depleted FMC medium. (B and C) Growth of OG1RF wild-type, (p)ppGpp^0, and Δ*rel* Δ*relQ* Δ*codY* strains in whole blood (B) or serum (C). For each time point, aliquots were serially diluted and plated on TSA plates at selected time points for CFU enumeration. Graphs A to C show averages and standard deviations of results from at least three independent experiments. (D) Kaplan-Meier plots of survival rates of *G. mellonella* larvae injected with *E. faecalis* OG1RF or its derivatives. The Kaplan-Meyer plot is a representative of an experiment repeated three independent times.

of the (p)ppGpp^0 strain. To confirm that the connection between (p)ppGpp and CodY regulation also occurs in *E. faecalis*, we tested the ability of the (p)ppGpp^0, Δ*codY*, and (p)ppGpp^0 Δ*codY* strains to grow in media lacking isoleucine, a trait that is mediated by the (p)ppGpp/CodY network (24). Despite *E. faecalis* lacking several enzymes required to synthesize BCAA, plate titrations revealed that inactivation of *codY* alleviated the isoleucine auxotrophy of the (p)ppGpp^0 mutant (see Fig. S1 in the supplemental material). Complementation (*in trans*) of *codY* in the triple mutant restored the isoleucine auxotrophy, indicating that the canonical (p)ppGpp/CodY regulatory network is present in *E. faecalis*. We further validated the *codY* mutation by showing that transcription of *opp*, an oligopeptide permease with a bona fide CodY-binding box (26), was significantly induced in the Δ*codY* strain (Fig. S1). Additional characterization of the single Δ*codY* mutant indicated that this strain was indistinguishable from the parent strain in tests for growth in metal-depleted media or in whole blood and with respect to *G. mellonella* killing (Fig. S2). On the other hand, deletion of *codY* in the (p)ppGpp^0 background strain restored growth in Mn-depleted media and whole blood and restored the virulence in *G. mellonella* (Fig. 4). However, it did not restore growth of the (p)ppGpp^0 strain when both Fe and Mn were depleted from FMC or in serum (Fig. 4). These results suggest that the connection between (p)ppGpp and metal homeostasis and its relevance to virulence is partly associated with CodY.

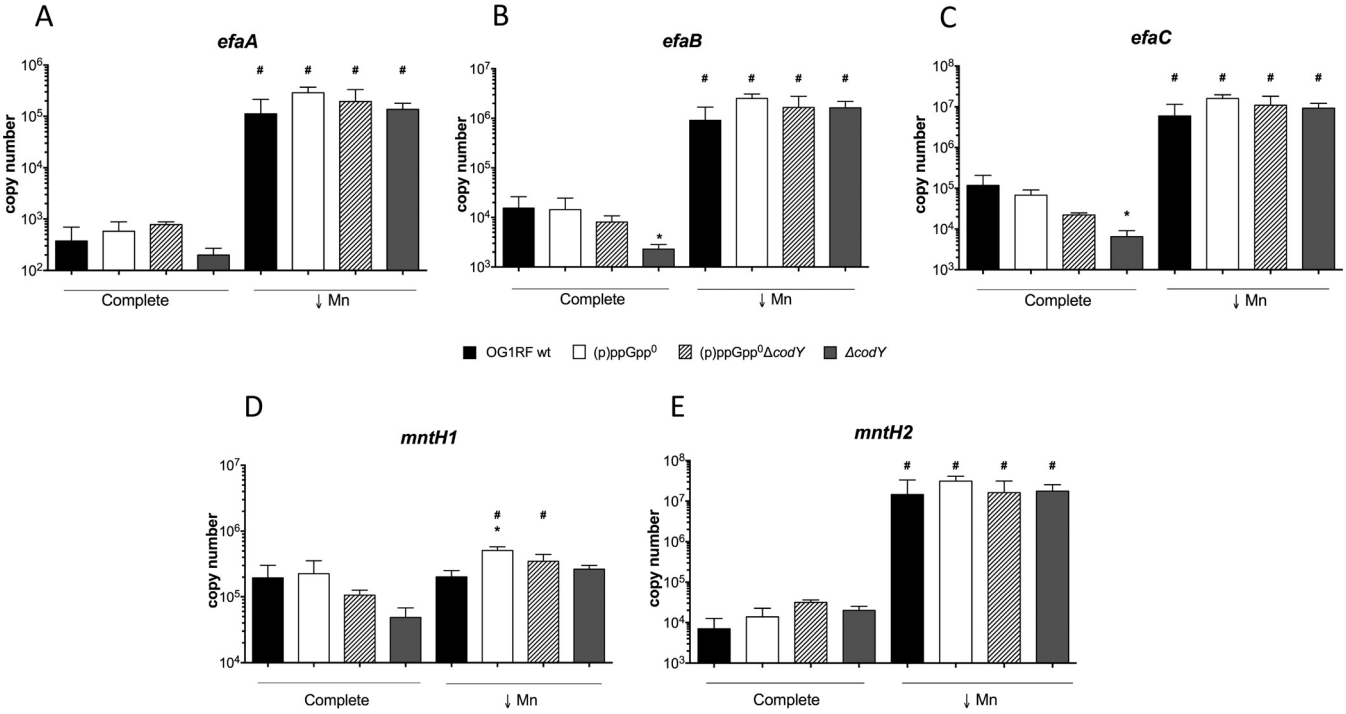

FIG 5 Transcription of *efaCBA*, *mntH1*, and *mntH2* during Mn limitation is not controlled by the (p)ppGpp/CodY regulatory network. The *E. faecalis* OG1RF wild-type, (p)ppGpp^0, and (p)ppGpp^0 Δ*codY* strains and Δ*codY* strain were grown in complete or Mn-depleted FMC medium to the mid-exponential growth phase, and transcript levels of *efaA* (A), *efaB* (B), *efaC* (C), *mntH1* (D), and *mntH2* (E) were determined by quantitative real-time PCR (qRT-PCR). The bar graphs show averages and standard deviations of results from three independent experiments performed in triplicate. Differences seen with the same strain under different conditions (#) or between parent and mutant strains under the same growth condition (*) were compared via Student's *t* test or ANOVA with Dunnett's posttest, respectively ($P \leq 0.05$).

(p)ppGpp and CodY are not involved in transcriptional regulation of known Mn transporters. The marked growth defect of the (p)ppGpp^0 strain under Mn-depleted conditions suggests two mutually nonexclusive explanations: (i) that lack of (p)ppGpp leads to a deficiency in Mn uptake and/or (ii) that lack of (p)ppGpp leads to an intrinsically higher cellular demand for Mn. Since (p)ppGpp typically activates transcription of nutrient transporters, we began to explore the first possibility by comparing the transcriptional profiles of the Mn uptake systems in the parent and (p)ppGpp^0 strains. The genome of OG1RF encodes three high-affinity Mn transporters: one ABC-type transporter (EfaCBA) and two natural resistance-associated macrophage protein (NRAMP)-type transporters, previously named MntH1 and MntH2 (27). Of note, the *efaA*, *mntH1*, and *mntH2* genes have been shown to be transcriptionally regulated by Mn availability (27, 28) and to be upregulated during growth in blood and urine *ex vivo*, as well as in a mouse peritonitis model (19, 20, 29). In agreement with those previous studies, transcription of *efaCBA* and *mntH2* was strongly (≥50-fold) induced under Mn-depleted conditions compared to the results seen with cells grown in metal-replete media, while induction of *mntH1* transcription did not change (Fig. 5). Irrespective of the Mn concentration in the media, transcription of these Mn transporters was largely unchanged in the (p)ppGpp^0 mutant compared to the parent strain. Indeed, only transcription of *mntH1* was slightly (2-fold) elevated in the (p)ppGpp^0 strain when Mn was depleted, but this small alteration is unlikely to be biologically relevant.

Even though (p)ppGpp does not appear to be involved in transcriptional control of high-affinity Mn uptake systems, inactivation of *codY* restored growth of the (p)ppGpp^0 strain in Mn-depleted media (Fig. 4A). Thus, it is conceivable that CodY regulates expression of metal transporters in a (p)ppGpp-independent manner. To test this possibility, we compared the transcriptional profiles of *efaCBA*, *mntH1*, and *mntH2* in the parent and (p)ppGpp^0 strains to those seen with the (p)ppGpp^0 Δ*codY* and Δ*codY* strains. Deletion of *codY* alone (Δ*codY*) or in the (p)ppGpp^0 background did not affect

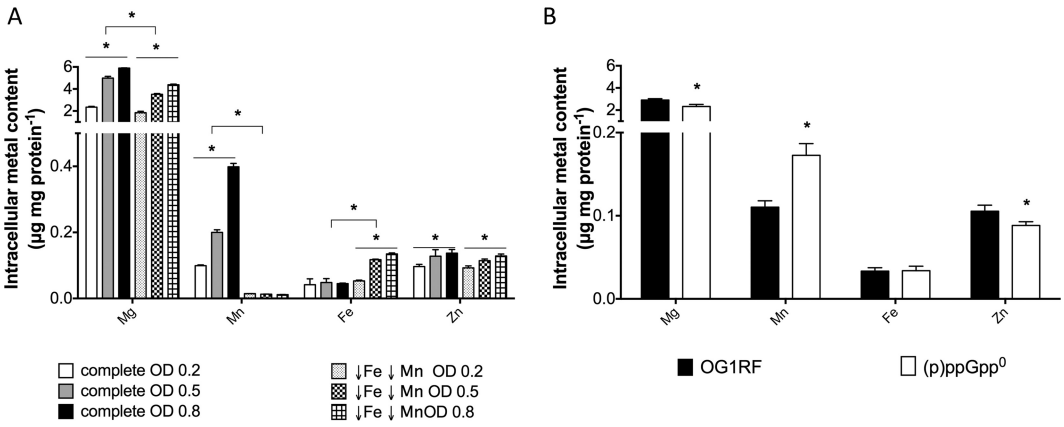

FIG 6 Intracellular metal content of *E. faecalis* OG1RF and (p)ppGpp^0 strains. (A) Intracellular metal quantifications of *E. faecalis* OG1RF strain during the early, mid-, and late-exponential-growth phases in metal-replete (complete) or metal-depleted (↓ Fe ↓ Mn) FMC medium. (B) Intracellular metal quantifications of *E. faecalis* OG1RF and (p)ppGpp^0 strains grown to mid-log phase (OD_{600}, ~0.5) in metal-replete FMC medium. The bar graphs show averages and standard deviations of results from three independent ICP-OES analyses (*, $P \leq 0.05$).

expression of any of the selected metal transporters during Mn depletion (Fig. 5), indicating that CodY was not compensating for the Mn dependence of the (p)ppGpp^0 strain by alleviating transcription of Mn uptake systems. In metal-replete media, the single Δ*codY* mutant displayed small decreases in *efaC* and *efaB* expression but these differences are unlikely to be biologically meaningful. Collectively, these results indicate that during Mn limitation, neither (p)ppGpp nor CodY regulates transcription of *efaCBA*, *mntH1*, and *mntH2*.

Intracellular Mn and Fe content shifts during metal limitation. Because the (p)ppGpp/CodY network was not involved in transcriptional regulation of *efaCBA*, *mntH1*, and *mntH2*, we wondered if lack of (p)ppGpp instead increases the cellular demand for Mn. First, we used ICP-OES to determine the total intracellular content of four biologically relevant transition metals (Mg, Mn, Fe, and Zn) in the parent strain under metal-replete growth conditions (FMC complete) during different growth phases. As expected for a "Mn-centric" organism, intracellular Mn pools increased significantly (up to 4-fold) during transition from the early log stage to the stationary phase (Fig. 6A). The level of intracellular Mg content followed the same trend and more than doubled during the transition from the early log phase to the stationary phase. Conversely, the levels of Fe and Zn remained relatively unchanged over the different growth phases (Fig. 6A). When cells were grown in media depleted for Fe and Mn, intracellular Mn levels were near the detection limit but the Fe levels were slightly elevated. This unexpected increase in intracellular Fe levels under conditions of Fe depletion could not be associated with the transcriptional activation of the two major Fe transport systems found in *E. faecalis*, as transcription of the ferrous iron transporter *feoB* gene and the ferrichrome permease *fhuG* gene did not change in response to metal starvation (Fig. S3). Considering that Fe uptake systems have not been properly characterized in *E. faecalis*, we cannot rule out the possibility that there are other, yet-to-be-identified Fe transporters that are induced under Fe-limiting conditions. It is noteworthy that the (p)ppGpp^0 strain showed an ~65% increase in the intracellular Mn level under metal-replete conditions, while the Fe levels were comparable to those seen with the parent strain (Fig. 6B). Despite Mn being an essential nutrient, high concentrations of Mn can be toxic to cells (30). Interestingly, the (p)ppGpp^0 mutant was also more sensitive to toxic concentrations of Mn than the wild-type strain (Fig. S4). While this might appear counterintuitive given that the (p)ppGpp^0 strain has a higher demand for Mn, this phenotype relates well to the global role of (p)ppGpp in cell growth and homeostasis and to the fact that lack of (p)ppGpp impairs metal homeostasis in *E. faecalis*.

The (p)ppGpp^0 strain has an elevated Mn requirement due to a dysregulated metabolism that increases ROS generation. During the SR, (p)ppGpp globally controls metabolic alterations necessary for survival under stress conditions (2). In *E. faecalis*, lack of (p)ppGpp severely affected the metabolic profile of the cell even in the absence of stress, resulting in a significant decrease in lactate production and a concomitant increase in the levels of formate, ethanol, and acetoin (18). As by-products of its metabolism, *E. faecalis* releases significant amounts of ROS, including superoxide and H_2O_2 (31, 32). We previously showed that the (p)ppGpp^0 strain produces ~5-fold more H_2O_2 during exponential growth, likely due to the uncontrolled metabolic flux of this strain (18). Given that (p)ppGpp does not appear to regulate Mn transporters (Fig. 5) and that lack of (p)ppGpp led to an increase in intracellular Mn levels (Fig. 6B), we asked whether the Mn dependence of the (p)ppGpp^0 strain is linked to the role of this biometal in mitigating ROS stress. First, we tested whether the (p)ppGpp^0 strain could grow more efficiently in Mn-depleted media under anaerobic incubation conditions. However, for unknown reasons, growth of the (p)ppGpp^0 strain was significantly impaired under anaerobiosis, regardless of the metal composition of the growth media (data not shown). Next, we evaluated the effect of two antioxidants, catalase and glutathione, on growth of the different strains under Mn-depleted or Fe-and-Mn-depleted conditions. While catalase did not rescue the growth defects of the (p)ppGpp^0 strain under metal-depleted conditions (data not shown), addition of reduced glutathione significantly improved its growth in Fe-and-Mn-depleted media and completely restored growth in Mn-depleted media (Fig. 7A). As expected, oxidized glutathione failed to restore growth of the (p)ppGpp^0 strain (Fig. 7C). To rule out metal contamination of the glutathione stock, the stock solution was subjected to ICP-OES analysis; the results confirmed that it was completely free of metal residues (data not shown). Given the very tight associations among Mn, SOD activity, and oxidative stress survival, we also measured SOD activity in both strains growing under metal-replete or metal-depleted conditions. Under Mn-depleted conditions or Fe-depleted conditions, the SOD activity in the parent strain was diminished ~22% ($P \geq 0.05$) or ~33% ($P \leq 0.05$), respectively (Fig. 7D), and was further reduced (~56%, $P \leq 0.05$) when both metals were depleted. The results showing the decrease in SOD activity during Mn depletion were supported by a significant decrease in *sodA* transcription under the same conditions (Fig. 7E). More importantly, the SOD activity of the (p)ppGpp^0 strain was significantly higher than that seen with the parent strain (~65% and ~25%, respectively) in cells grown under Fe-depleted conditions or Mn-depleted conditions ($P \leq 0.05$). Because the (p)ppGpp^0 strain cannot grow under Fe-and-Mn-limiting conditions, we were unable to measure SOD activity of this strain under these conditions. The increase in SOD activity of the (p)ppGpp^0 strain supported the notion that this strain requires additional Mn to cope with intrinsically generated ROS stress. To further confirm that the (p)ppGpp^0 strain continues to produce more ROS in the absence of Fe or Mn, we quantified H_2O_2 production under metal limitation conditions. In agreement with previous findings (18), the (p)ppGpp^0 strain generated ~5-fold more H_2O_2 than the parent strain in metal-replete media. Remarkably, the mutant strain maintained elevated H_2O_2 levels under all conditions, mirroring its SOD activity (Fig. 7F). Collectively, these results strongly indicate that the (p)ppGpp^0 strain requires larger amounts of Mn to cope with intrinsically generated ROS.

Inactivation of *codY* restores a balanced metabolism in the absence of (p)ppGpp. It is intriguing that inactivation of *codY*, a BCAA- and GTP-sensing transcriptional regulator, restored several phenotypes of the (p)ppGpp^0 strain without having an obvious impact on transcription of the Mn transporters (Fig. 4 and 5). Interestingly, ICP-OES analysis revealed that the intracellular Mn content of the (p)ppGpp^0 Δ*codY* strain grown in metal-replete medium was identical to that seen with the parent strain (Fig. 8A), suggesting that alleviation of CodY regulation restores the imbalanced metal homeostasis and, more specifically, the (p)ppGpp-dependent cellular Mn requirement of the (p)ppGpp^0 mutant. In agreement with this, deletion of *codY* significantly ameliorated the H_2O_2 production of the (p)ppGpp^0 strain (Fig. 8B). Previously, we showed

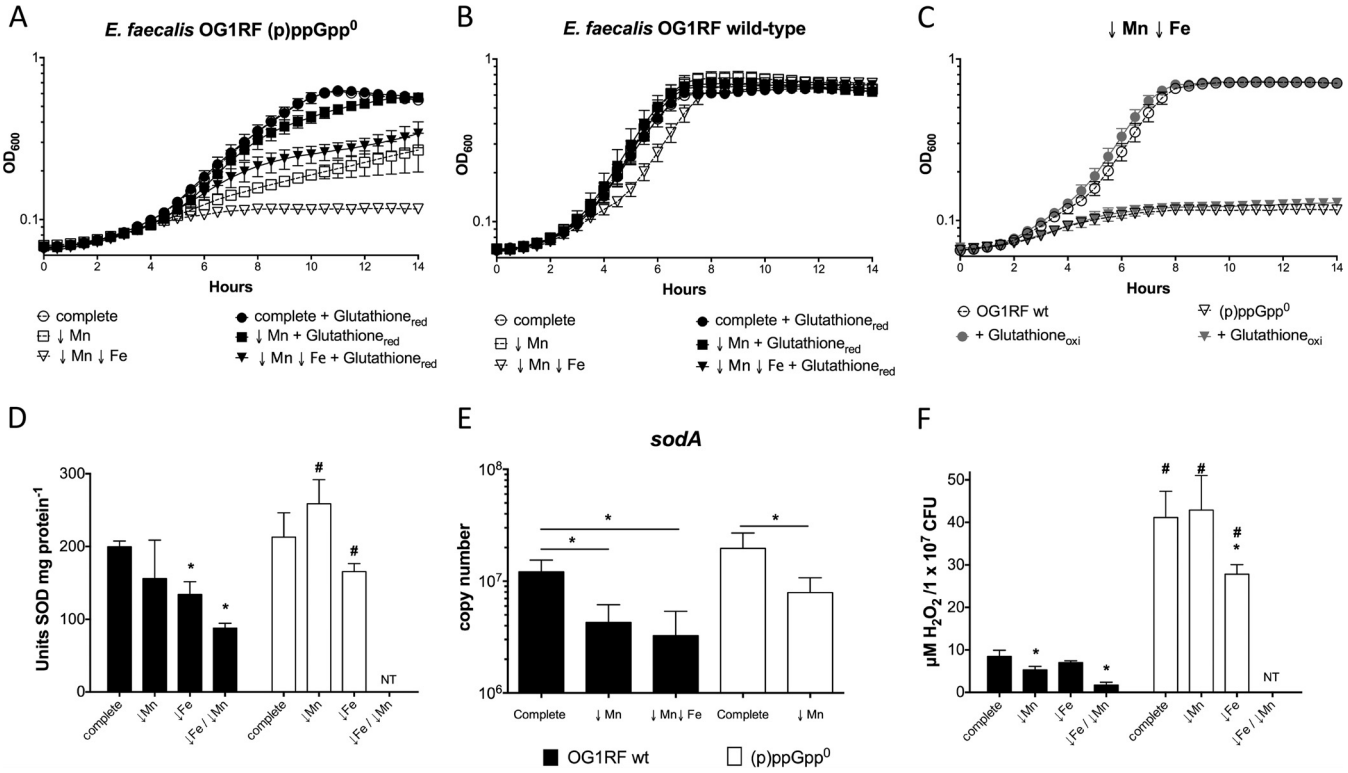

FIG 7 The (p)ppGpp^0 strain has a strong Mn requirement due to elevated ROS generation. (A to C) Growth of *E. faecalis* (p)ppGpp^0 (A) and OG1RF wild-type (B) strains in complete, Mn-depleted, or Fe/Mn-depleted FMC medium in the presence or absence of 1 mM reduced glutathione. (C) Growth of the (p)ppGpp^0 strain in metal-depleted FMC medium in the presence of oxidized glutathione. (D) Quantification of SOD activity in OG1RF and (p)ppGpp^0 strains. Cells were grown to an OD_{600} of ~0.3 in FMC medium depleted of Fe or Mn or both and were harvested by centrifugation. Cells were then lysed, serially diluted, and tested for SOD activity using the cytochrome *c*, xanthine, xanthine oxidase method. (E) Transcriptional expression of *sodA* in response to Mn depletion. The *E. faecalis* OG1RF wild-type and (p)ppGpp^0 strains were grown in complete, Mn-depleted, or Fe-and-Mn-depleted FMC medium to the mid-exponential-growth phase, and transcript levels of *sodA* were determined by qRT-PCR. The bar graphs show averages and standard deviations of results from three independent experiments performed in triplicate. Differences among strains and under different conditions were compared via Student's *t* test ($P \leq 0.05$). (F) H_2O_2 production in OG1RF and (p)ppGpp^0 strains. Cells were grown to an OD_{600} of ~0.3 in FMC medium depleted of Fe or Mn or both and were harvested by centrifugation. Then, cells were washed in $NaPO_4$ buffer, mixed with Amplex red solution, and incubated for 30 min before H_2O_2 determination. The graphs show averages and standard deviations of results from at least three independent experiments. Differences seen with the same strain under different conditions (*) or between parent and (p)ppGpp^0 strains under the same condition (#) were compared ($P \leq 0.05$). NT, not tested.

that lack of (p)ppGpp in *E. faecalis* leads to a switch from homolactic fermentation to heterolactic fermentation, leading to a significant increase in production of nonacidic acetoin. This can be validated by the inability of the (p)ppGpp^0 strain to reduce the culture pH to wild-type levels (18). The (p)ppGpp^0 Δ*codY* mutant strain was able to acidify the media to the same extent as the parent strain (Fig. 8C), further supporting the notion that removing CodY regulation restores, at least in part, the dysregulated metabolism of the (p)ppGpp^0 strain.

DISCUSSION

We have previously shown that the inability to synthesize (p)ppGpp negatively affects the pathophysiology of *E. faecalis*. Specifically, the (p)ppGpp^0 strain displays increased sensitivity to macrophages, impaired growth and survival in serum or whole blood, and attenuated virulence in animal models (6–8). In this report, we show that these phenotypes are intimately associated with metal homeostasis. Specifically, addition of either Fe or Mn alone was sufficient to restore growth of the (p)ppGpp^0 mutant in serum. While Fe supplementation increased growth rates and yields of *E. faecalis* in a (p)ppGpp-independent manner, Mn restored growth of the (p)ppGpp^0 mutant without any visible physiologic consequence with respect to the parent strain. This result confirms that, similarly to other pathogens, Fe is a major growth-limiting factor for *E. faecalis* during invasive infections (17, 33, 34). The biological significance of this observation is underscored by the high incidence of opportunistic infections in indi-

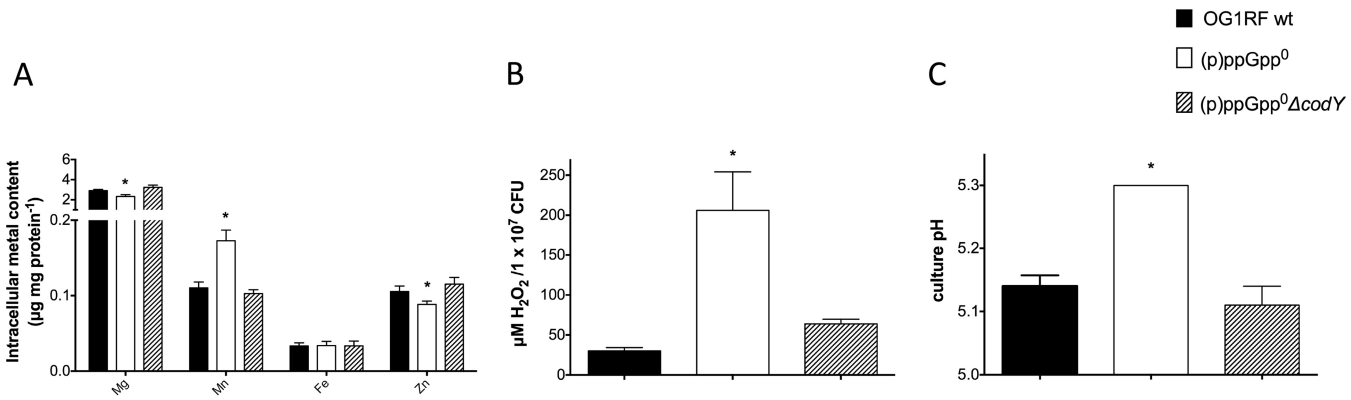

FIG 8 Deletion of *codY* in the (p)ppGpp^0 background restores intracellular metal accumulation, H_2O_2 production, and culture acidification. (A) Intracellular metal quantifications of *E. faecalis* OG1RF, (p)ppGpp^0, and (p)ppGpp^0 Δ*codY* strains grown to mid-log phase (OD_{600}, ~0.5) in metal-replete FMC medium. The bar graphs show averages and standard deviations of results from three independent ICP-OES analyses (*, $P \leq 0.05$). (B) Quantification of H_2O_2 production in OG1RF, (p)ppGpp^0, and (p)ppGpp^0 Δ*codY* strains. Cells were grown to an OD_{600} of ~0.3 in FMC medium depleted of Mn and were harvested by centrifugation. Then, cells were washed twice in $NaPO_4$ buffer, mixed with Amplex red solution, and incubated for 30 min before H_2O_2 determination. The graphs show averages and standard deviations of results from six independent experiments (*, $P \leq 0.05$). (C) For pH determination, cells were grown to late log phase in FMC complete medium and culture pH was immediately recorded.

viduals with high levels of circulating free Fe, as seen in patients with hemochromatosis and other iron-related disorders (17). The biological significance of Mn is much less understood, but data from studies from the Skaar laboratory and others that were performed using calprotectin and Mn transport mutants indicate that chelation of Mn is biologically (and medically) important (35, 36). Notably, depletion of both metals in the laboratory media, mimicking the metal restriction found in host tissues, completely halted cell growth of the (p)ppGpp^0 strain, stressing the overlapping functions of these two metals. It is noteworthy that the linkage between (p)ppGpp and metal homeostasis is not restricted to *E. faecalis* strains, as studies performed with the human respiratory pathogen *Streptococcus pneumoniae* reported a similar Mn growth requirement in a (p)ppGpp-deficient strain (37).

Although the data are not as robust as those representing amino acid starvation, we showed for the first time that depletion of either Mn or Fe led to an increase in (p)ppGpp pools in *E. faecalis*. Modest increases in (p)ppGpp levels (below those needed to activate the SR) have been shown to contribute to restoration of cellular homeostasis under mildly stressful conditions (3). It is thus possible that slight increases in levels of (p)ppGpp during metal limitation allow metabolic fine-tuning to match the cellular metal requirement to the metal availability. Because the genomes of *E. faecalis* strains encode two (p)ppGpp synthetases, Rel and RelQ, we used thin-layer chromatography (TLC) to demonstrate that the bifunctional Rel is the enzyme responsible for (p)ppGpp accumulation during metal limitation. However, it remains to be determined how Rel senses this stress. It was suggested previously that Fe limitation in *B. subtilis* indirectly leads to amino acid starvation, as several amino acid biosynthetic enzymes use Fe as a cofactor (38). Even though transcription of *rel* does not change during Mn limitation (see Fig. S3 in the supplemental material), Rel is known to use Mn as the required cofactor during (p)ppGpp hydrolysis (39, 40). Therefore, it is tempting to speculate that (p)ppGpp synthetized by RelQ or Rel itself would steadily accumulate due to the presence of a poorly active or inactive Rel hydrolase. Finally, it is also possible that Rel directly and specifically senses metal starvation, thereby acquiring a conformation that favors (p)ppGpp synthesis over degradation. The precise mechanisms explaining how Rel senses Fe and Mn limitation warrant further investigations.

The genome of OG1RF, our working *E. faecalis* strain, encodes at least three Mn transporters, namely, the ABC-type EfaCBA permease and two NRAMP-type transporters named MntH1 and MntH2 (27). Transcriptional studies revealed that (p)ppGpp does not regulate expression of the *efaCBA*, *mntH1*, and *mntH2* genes, at least under the conditions tested. This was also the case in *S. pneumoniae*, where metal uptake systems

were not regulated by (p)ppGpp (37). Nevertheless, ICP-OES analysis provided several important clues into how *E. faecalis* accumulates and balances biometals and how changes in Mn and Fe availability may dictate the fate of the (p)ppGpp^0 strain. As observed in other lactic acid bacteria, intracellular Mn levels increased in a growth-phase-dependent manner and cells accumulated 9-fold more Mn than Fe before reaching the stationary phase (Fig. 6) (13, 14). This is in agreement with the knowledge that lactic acid bacteria preferentially utilize the relatively innocuous Mn instead of the highly reactive Fe during ROS stress (15). Notably, while it is well established that Fe depletion in the presence of ROS minimizes cell damage due to Fenton chemistry, the central role of Mn in oxidative stress tolerance is underscored by the observation that *E. faecalis* is unable to grow in the presence of subinhibitory concentrations of H_2O_2 when Mn is depleted (Fig. S5A). Interestingly, under conditions of severe metal limitation, the parent strain displayed normal growth rates and yields despite having ~30 times less intracellular Mn. Furthermore, this dramatic drop in Mn content was accompanied by a 3-fold increase in Fe content, suggesting that *E. faecalis* compensates for lower levels of Mn by taking up additional Fe. While this appears counterintuitive, it is well known that Fe and Mn can act as interchangeable enzymatic cofactors (30, 41).

On the basis of the ability of reduced glutathione levels to rescue growth of the (p)ppGpp^0 strain under Mn-depleted conditions, we can conclude that its higher Mn requirement is directly linked to oxidative stress. We have previously shown that lack of (p)ppGpp leads to a dysregulated metabolism, which in turn results in a shift from homolactic fermentation to a heterofermentative mode and in significant increases in ROS production (18). In principle, to cope with high levels of intrinsically generated ROS, the (p)ppGpp^0 strain requires higher intracellular concentrations of Mn. Accordingly, the (p)ppGpp^0 strain accumulated 65% more Mn than the parent strain when Mn was provided in the growth media. Of note, even small increases in intracellular Mn levels can significantly alter the activity of several metabolic enzymes, including those that contribute to central carbon flux (13, 42). Because the (p)ppGpp^0 strain is unable to maintain a balanced metabolism, it produces significantly larger amounts of H_2O_2 and superoxide as by-products of its normal metabolism (Fig. 9). This, in turn, inevitably leads to ROS damage and growth arrest. To counteract this intrinsically generated ROS stress, the (p)ppGpp^0 strain displayed higher levels of MnSOD activity, thereby increasing the cellular demand for Mn.

The main sources of ROS in *E. faecalis* are oxidative metabolism of glycerol and incomplete demethylmenaquinone reduction during the activity of the electron transport chain in the absence of heme (31, 32). Since the FMC media lack both glycerol and heme, we speculated that the majority of H_2O_2 produced under these conditions derives from the incomplete electron transport chain and subsequent superoxide dismutation by MnSOD. However, heme supplementation did not restore growth of the (p)ppGpp^0 strain in Mn-depleted media (Fig. S5B and C). Therefore, it is possible that the (p)ppGpp^0 strain has a defect in heme utilization, has additional defects in the electron transport chain, or has other ROS-generating pathways.

Though it might seem counterintuitive given the Fe-mediated Fenton reaction, Fe depletion exacerbated the Mn dependence of the (p)ppGpp^0 strain. While glutathione completely restored growth of the (p)ppGpp^0 strain under Mn-depleted conditions, it restored growth only partially when both Mn and Fe were limiting, further indicating that Fe depletion poses an additional stress. Moreover, SOD activity of *E. faecalis* was lower during Fe limitation in both the parent and mutant strains. It is thus possible that an imbalance in intracellular Fe/Mn ratios caused by Fe depletion titrates Mn ions away from the Mn-dependent SOD in order to support the activity of essential enzymes. Regardless of the underlying mechanism that dictates this decrease in SOD activity, we cannot rule out the possibility that low Fe and Mn availability has additional deleterious effects on growth of the (p)ppGpp^0 strain.

The correlation between (p)ppGpp levels and CodY activity in a variety of *Firmicutes* species is firmly established (24), and CodY has been associated with Fe homeostasis by

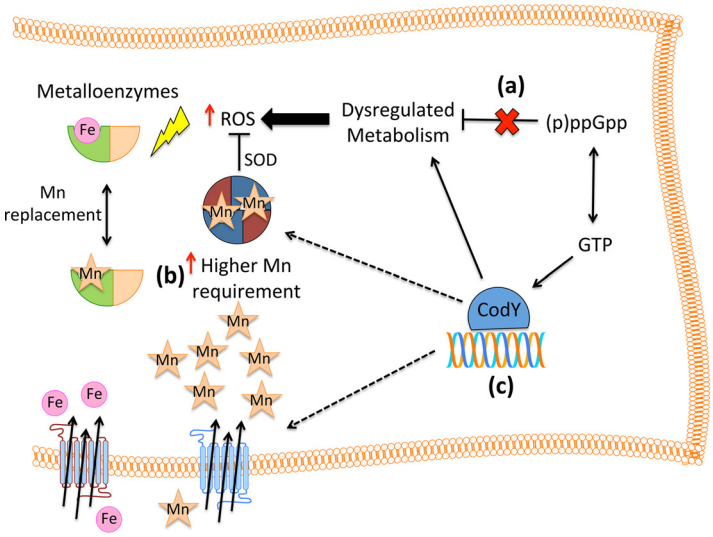

FIG 9 Dysregulated metabolism of the (p)ppGpp^0 strain leads to high Mn requirement. In *E. faecalis*, endogenous ROS derives from an active metabolism. (a) In the absence of (p)ppGpp, a highly dysregulated metabolism leads to significant increases in ROS production (18). (b) The (p)ppGpp^0 strain requires higher intracellular Mn levels to cope with increased ROS production. Manganese contributes to detoxification by acting as the optimal SOD cofactor and by serving as the surrogate cofactor for several Fe-binding enzymes (9). (c) Reductions in intracellular GTP pools due to (p)ppGpp accumulation result in less-stable CodY-DNA interactions, thereby alleviating CodY regulation (24). Inactivation of *codY* in the (p)ppGpp^0 background restored growth under Mn-depleted conditions but not under Mn- and Fe-depleted conditions. We propose that CodY restores Mn homeostasis in the (p)ppGpp^0 mutant by restoring several dysregulated metabolic pathways, thus reducing ROS production and the accompanying Mn requirement. Other possible mechanisms include the following: (i) CodY functions as a negative regulator of a yet-to-be-identified metal transporter(s) (43, 44) or (ii) CodY directly represses transcription of oxidative stress genes or (iii) CodY affects low-molecular-weight (LMW) metal complexes, thereby affecting Mn and Fe availability (14). In the absence of both Mn and Fe, SOD activity is dramatically impaired and alleviation of CodY regulation can no longer compensate for the loss of (p)ppGpp.

acting as an activator of Fe acquisition genes in *Bacillus anthracis* and as a repressor in *S. pneumoniae* (43, 44). At first glance, the logical explanation for the partial restoration of the (p)ppGpp^0 strain phenotypes upon *codY* deletion is that CodY represses, in a (p)ppGpp-independent manner, transcription of a gene(s) coding for a metal transporter(s). However, deletion of *codY* alone or in the (p)ppGpp^0 background strain had no obvious impact on transcription of *efaCBA*, *mntH1*, and *mntH2* (Fig. 5). As previously mentioned, (p)ppGpp and CodY cooperate to broadly orchestrate bacterial metabolism in response to nutritional cues (24). To begin to determine if inactivation of CodY restores the unbalanced metabolic flux of the (p)ppGpp^0 strain, we compared the ability of the triple mutant strain to generate H_2O_2 and acidify the growth culture to that of the parent and (p)ppGpp^0 strains. Indeed, the (p)ppGpp^0 Δ*codY* mutant strain generated similar amounts of H_2O_2 and was able to acidify the media to the same extent as the parent strain (Fig. 8), supporting the notion that removing CodY repression restores the dysregulated metabolism of the (p)ppGpp^0 strain. While exactly how CodY restores (p)ppGpp-associated phenotypes remains to be determined, there are a few possibilities that should be considered in regard to metal homeostasis (Fig. 9). For instance, metabolic rearrangements due to lack of CodY control may affect the intracellular concentrations of low-molecular-weight (LMW) metal complexes such as amino acids and nucleotides, thereby affecting free metal pools (14). Alternatively, the CodY regulon might also include oxidative stress tolerance genes or other metal uptake systems necessary to protect the (p)ppGpp^0 strain against ROS by-products. In the near future, transcriptome and metabolome analyzes should be used to obtain a mechanistic understanding of the role of CodY, and its relationship with (p)ppGpp-related phenotypes, in metal homeostasis.

Collectively, our results revealed that the (p)ppGpp^0 strain depends on high levels

TABLE 1 Bacterial strains used in this study

Strains	Relevant characteristic(s)[a]	Source
E. faecalis		
OG1RF	Reference sequenced strain; Rif^r Fus^r	Laboratory stock
Δrel_{Ef}	High basal (p)ppGpp; SR negative[b]	6
Δ$relQ_{Ef}$	Delayed SR[b]	6
Δrel_{Ef} Δ$relQ_{Ef}$	(p)ppGpp^0[b]	6
Δ*codY*	*codY* deletion	This study
Δrel_{Ef} Δ$relQ_{Ef}$ Δ*codY*	(p)ppGpp^0, *codY* deletion	This study
Δ*codY* + *pcodY*		This study
Δrel_{Ef} Δ$relQ_{Ef}$ Δ*codY* + *pcodY*		This study
V583	Reference sequenced strain	22
V583 Δrel_{Ef} Δ$relQ_{Ef}$	(p)ppGpp^0	22
CK111	OG1Sp *upp4*::P23*repA4*	47
E. coli		
EC1000	Host for RepA-dependent plasmids	48

[a]Fus^r, fusidic acid resistance; Rif^r, rifampin resistance.
[b]For details, see Gaca et al. (7).

of intracellular Mn to protect itself against endogenously produced ROS. There are, however, important questions that remain unanswered. How does the interchangeable nature of Fe and Mn affect cell homeostasis? Given that (p)ppGpp accumulates during Fe or Mn starvation and that inactivation of CodY restores growth in Mn-depleted media, which metabolic pathways does the (p)ppGpp/CodY network directly regulate during metal stress? As we devote our future efforts to unraveling the molecular mechanisms linking (p)ppGpp to metal homeostasis, the findings presented in this study will have immediate and broad implications. The prominent role of (p)ppGpp regulation in the virulence of a number of bacterial pathogens and in antibiotic persistence has been extensively documented (3–5), and compounds that interfere with (p)ppGpp signaling have been identified (45, 46). It will be interesting to learn whether the associations among (p)ppGpp, metal homeostasis, and virulence in *E. faecalis* also occur in other bacterial pathogens and whether the associations can be further explored to develop new anti-infective approaches.

MATERIALS AND METHODS

Bacterial strains. Bacterial strains used in this study are listed in Table 1. The parent *E. faecalis* OG1RF strain and the corresponding derivative Δ*rel*, Δ*relQ*, and Δ*rel* Δ*relQ* [(p)ppGpp^0] strains have been previously described (6). The *E. faecalis* V583 wild-type and (p)ppGpp^0 strains were generously provided by Axel Hartke at the University of Caen (22). All *E. faecalis* strains, including those generated in this study (see below), were routinely grown in brain heart infusion (BHI) broth overnight at 37°C.

Construction of Δ*codY* and (p)ppGpp^0 Δ*codY* strains. The pCJK47 markerless genetic exchange system was used to delete *codY* from the *E. faecalis* OG1RF and Δ*rel* Δ*relQ* strains (47). Briefly, two PCR products flanking the *codY* coding sequence were obtained with the primers listed in Table S1 in the supplemental material. The amplicons were approximately 1 kb in size and included the first 30 and last 34 residues of the *codY* coding DNA, which were retained to avoid unanticipated effects on the expression of adjacent genes. After digestion with the appropriate restriction enzymes, the DNA products flanking the gene of interest were cloned into pCJK47 using *E. coli* EC1000 as the host strain. The resulting plasmid was electroporated into competent *E. faecalis* CK111 (donor strain). Subsequently, CK111 harboring plasmid pCJK-*codY* was conjugated with the OG1RF and Δ*rel* Δ*relQ* strains, and single-crossover insertions were selected on BHI agar containing rifampin and erythromycin. Single colonies were subjected to the PheS* negative counterselection system to isolate double-crossover deletions as described elsewhere (47). The *codY* deletion was confirmed by PCR sequencing of the insertion site and flanking sequences.

The rhamnose-inducible pCJK96 plasmid (49) was used to complement the Δ*codY* and (p)ppGpp^0 Δ*codY* strains. Briefly, the *codY* coding sequence was amplified using the primers listed on Table S1 and was cloned into pCJK96 to yield plasmid pcodY-comp. The plasmid was electroporated into the Δ*codY* strains using standard protocols (49).

Growth kinetic assays. Growth in horse serum (Lonza) or human whole blood and serum (University of Rochester Medical Center blood bank) was monitored as described elsewhere (8). Where indicated, serum was supplemented with a final concentration of 1 mM $FeSO_4$ (99%, Sigma), $MnSO_4$ (99%, Sigma), or $ZnSO_4$ (99.5%, Acros Organics). The chemically defined FMC medium was used as a means to control the metal concentration (50). Omission of $FeSO_4$ or $MnSO_4$ or both metals during preparation of FMC robustly depleted these metals to levels in the low nanomolar range (see results). Metal contamination

was avoided by using reagent-grade H_2O (Thermo Scientific) and by soaking glassware, stirrers, and plastic vessels overnight in a 1 M trace-metal-grade HNO_3 acid bath prior to use. To assess the ability of the strains to grow in metal-depleted media, overnight cultures were diluted 1:40 in complete FMC and allowed to reach exponential growth (optical density at 600 nm [OD_{600}], ~0.25). At that point, cultures were diluted 1:100 into fresh FMC medium depleted for Fe or Mn or both and growth at 37°C was monitored using the Bioscreen growth reader (Oy growth curves; AB Ltd.). When indicated, 2 mM $MnSO_4$, 1 mM reduced (PanReac) or oxidized (Aldrich) glutathione, or 5 μM heme (Sigma) was added to the culture prior to growth monitoring.

ICP-OES. Total metal concentrations in the FMC medium preparations and within bacterial cells were determined by inductively coupled plasma-optical emission spectrometry (ICP-OES) at the University of Florida Institute of Food and Agricultural Sciences Analytical Services Laboratories. For quantification of metals in medium preparations, 2 ml trace-metal-grade 35% HNO_3 was added to 18 ml FMC media prior to analysis. For determination of intracellular metal content in strains during growth, prewarmed FMC media with or without added Fe and Mn was inoculated 1:20 with an overnight culture and incubated statically at 37°C. At selected growth-phase time points, aliquots were collected for metal analysis and total protein determination. Cells were harvested by centrifugation at 4°C for 15 min at 4,000 rpm and washed twice in ice-cold phosphate-buffered saline (PBS) supplemented with 0.5 mM EDTA to chelate extracellular divalent cations. Then, bacterial pellets were resuspended in 1 ml 35% HNO_3 and digested at 90°C for 1 h in a high-density polyethylene scintillation vial (Fisher Scientific). Digested bacteria were diluted 1:10 in reagent-grade H_2O prior to ICP-OES metal analysis. Metal composition was quantified using a 5300DV ICP atomic emission spectrometer (PerkinElmer), and concentrations were determined by comparisons to a standard curve. Metal concentrations were normalized to total protein content determined by the bicinchoninic acid (BCA) assay.

Detection of (p)ppGpp accumulation. Overnight cultures of OG1RF, Δ*rel*, Δ*relQ*, and Δ*rel* Δ*relQ* strains were washed once in metal-depleted FMC medium and diluted 1:40 in fresh, low-phosphate FMC medium (complete, Fe depleted, Mn depleted, or Fe and Mn depleted). As a positive control, OG1RF grown in FMC complete was treated with 50 μg ml^{-1} mupirocin for 30 min, a condition previously shown to immediately trigger robust accumulation of (p)ppGpp (6). Cells were grown to an OD_{600} of ~0.25 and were labeled with 100 μCi ml^{-1} carrier-free [^{32}P]orthophosphate (PerkinElmer) for 45 min. At this point, nucleotide pools were extracted with 50 μl ice-cold 3 M formic acid, followed by two freeze-thaw cycles. Acid extracts were briefly centrifuged, and supernatants were spotted onto polyethyleneimine (PEI)-cellulose plates (Millipore) for separation by thin-layer chromatography (TLC) in 1.25 M KH_2PO_4 (pH 3.4). Reaction products were visualized using a phosphorimager (Molecular Imager FX; Bio-Rad).

***Galleria mellonella* infection.** Assessment of virulence of OG1RF, Δ*codY*, (p)ppGpp^0, and (p)ppGpp^0 Δ*codY* strains in larvae of *G. mellonella* was performed as described elsewhere (7). Briefly, groups of 20 larvae, ranging from 200 to 300 mg in weight, were randomly chosen and injected with 5 μl aliquots of bacterial inoculum (5×10^5 CFU). Groups injected with heat-inactivated *E. faecalis* OG1RF (20 min at 75°C) were used as negative controls. After injection, larvae were kept at 37°C, and survival was recorded at selected intervals. Experiments were performed independently three times with similar results.

RNA extraction and real-time quantitative PCR. Overnight cultures were diluted 1:40 in 5 ml FMC complete or FMC depleted for Mn and allowed to grow statically at 37°C to an OD_{600} of 0.45. At that point, cultures were mixed with an equal volume of ice-cold ethanol/acetone solution (1:1), immediately frozen in a dry ice/ethanol bath, and kept at −80°C until ready for RNA extraction. Cells were then harvested, washed twice in TE buffer (10 mM Tris-Cl [pH 8], 1 mM EDTA), and digested with 25 U mutanolysin and 10 mg ml^{-1} lysozyme for 30 min at 37°C. Protoplasts were lysed with vigorous vortex mixing in 0.35 ml RLT buffer (Qiagen) supplemented with 1% β-mercaptoethanol, and RNA was purified using an RNeasy minikit (Qiagen), including the on-column DNase treatment recommended by the supplier. To further reduce DNA contamination, RNA samples were treated with DNase I (Ambion) at 37°C for 30 min and were repurified using an RNeasy minikit (Qiagen). RNA concentrations were determined using a NanoVue Plus spectrophotometer (GE Life Sciences). Reverse transcription and real-time PCR were carried out according to protocols described previously (51) using the indicated primer sets (Table S1).

Oxidative stress assays. Superoxide dismutase (SOD) activity was measured by the cytochrome *c*, xanthine, xanthine oxidase method (52). Briefly, overnight cultures were washed in metal-depleted FMC, diluted 1:40, and grown to an OD_{600} of 0.3 in FMC medium with or without added Fe and/or Mn. Then, cells were harvested by centrifugation, washed twice, and resuspended in 0.5 ml sterile 25 mM Tris buffer (pH 8). An equal volume of acid-washed 0.1 mm diameter glass beads was added, and the mixture was homogenized in a Bead Beater for four 30-s intervals. Homogenized cells were then centrifuged for 20 min at 4°C, and the fresh clear lysates were used to quantify SOD activity. Cell lysates were sequentially diluted, and SOD activity was determined by the use of a SOD assay kit following the instructions of the manufacturer (Sigma-Aldrich). Protein concentrations of cell lysates were determined by the BCA assay, and SOD activity was normalized to the total protein concentration. Production of H_2O_2 was measured using an Amplex red H_2O_2/peroxidase assay kit (Life Technologies) as described elsewhere (18). To normalize fluorescence by CFU, cell aliquots were serially diluted and plated onto tryptic soy agar (TSA) plates for CFU enumeration.

Statistical analysis. Data were analyzed using GraphPad Prism 6.0 software. Growth curves were statistically analyzed via a two-way analysis of variance (ANOVA) followed by Dunnett's comparison posttest. (p)ppGpp spots were quantified using the Image J image analysis tool, and statistical significance was assessed via one-way ANOVA followed by Dunnett's posttest. Differences in levels of metal accumulation between strains or between metal-replete and metal-depleted media, as well as differ-

ences in SOD activity and H_2O_2 production between strains, were determined via Student's *t* test. Depletion of Fe and/or Mn of the different FMC media, growth-phase-dependent changes in levels of metal accumulation, and differences in levels of gene expression (>2-fold difference) as well as in SOD activity and H_2O_2 production in response to metal availability were analyzed via one-way ANOVA followed by Dunnett's posttest. Survival rates of larvae were compared using the Mantel-Cox log-rank test. All experiments were repeated at least three times, and *P* values of ≤0.05 were considered statistically significant.

SUPPLEMENTAL MATERIAL

Supplemental material for this article may be found at https://doi.org/10.1128/IAI.00260-17.

SUPPLEMENTAL FILE 1, PDF file, 2.7 MB.

ACKNOWLEDGMENTS

The *E. faecalis* V583 and V583-(p)ppGpp⁰ strains were kindly provided by Axel Hartke, University of Caen, Caen, France. We thank Jacqueline Abranches and Jessica Kajfasz for critical reading of the manuscript.

C.C.-W. was supported by an American Heart Association GSA Predoctoral Fellowship (16PRE29860000). A.O.G. was supported by the NIDCR training program in oral science (T90 DE021985). The funders had no role in study design, data collection and interpretation, or the decision to submit the work for publication.

REFERENCES

1. Arias CA, Murray BE. 2012. The rise of the *Enterococcus*: beyond vancomycin resistance. Nat Rev Microbiol 10:266–278. https://doi.org/10.1038/nrmicro2761.
2. Potrykus K, Cashel M. 2008. (p)ppGpp: still magical? Annu Rev Microbiol 62:35–51. https://doi.org/10.1146/annurev.micro.62.081307.162903.
3. Gaca AO, Colomer-Winter C, Lemos JA. 2015. Many means to a common end: the intricacies of (p)ppGpp metabolism and its control of bacterial homeostasis. J Bacteriol 197:1146–1156. https://doi.org/10.1128/JB.02577-14.
4. Hauryliuk V, Atkinson GC, Murakami KS, Tenson T, Gerdes K. 2015. Recent functional insights into the role of (p)ppGpp in bacterial physiology. Nat Rev Microbiol 13:298–309. https://doi.org/10.1038/nrmicro3448.
5. Dalebroux ZD, Svensson SL, Gaynor EC, Swanson MS. 2010. ppGpp conjures bacterial virulence. Microbiol Mol Biol Rev 74:171–199. https://doi.org/10.1128/MMBR.00046-09.
6. Abranches J, Martinez AR, Kajfasz JK, Chavez V, Garsin DA, Lemos JA. 2009. The molecular alarmone (p)ppGpp mediates stress responses, vancomycin tolerance, and virulence in *Enterococcus faecalis*. J Bacteriol 191:2248–2256. https://doi.org/10.1128/JB.01726-08.
7. Gaca AO, Abranches J, Kajfasz JK, Lemos JA. 2012. Global transcriptional analysis of the stringent response in *Enterococcus faecalis*. Microbiology 158:1994–2004. https://doi.org/10.1099/mic.0.060236-0.
8. Frank KL, Colomer-Winter C, Grindle SM, Lemos JA, Schlievert PM, Dunny GM. 2014. Transcriptome analysis of *Enterococcus faecalis* during mammalian infection shows cells undergo adaptation and exist in a stringent response state. PLoS One 9:e115839. https://doi.org/10.1371/journal.pone.0115839.
9. Papp-Wallace KM, Maguire ME. 2006. Manganese transport and the role of manganese in virulence. Annu Rev Microbiol 60:187–209. https://doi.org/10.1146/annurev.micro.60.080805.142149.
10. Messenger AJM, Barclay R. 1983. Bacteria, iron and pathogenicity. Biochem Educ 11:54–63. https://doi.org/10.1016/0307-4412(83)90043-2.
11. Kehl-Fie TE, Skaar EP. 2010. Nutritional immunity beyond iron: a role for manganese and zinc. Curr Opin Chem Biol 14:218–224. https://doi.org/10.1016/j.cbpa.2009.11.008.
12. Touati D. 2000. Iron and oxidative stress in bacteria. Arch Biochem Biophys 373:1–6. https://doi.org/10.1006/abbi.1999.1518.
13. Kehres DG, Maguire ME. 2003. Emerging themes in manganese transport, biochemistry and pathogenesis in bacteria. FEMS Microbiol Rev 27:263–290. https://doi.org/10.1016/S0168-6445(03)00052-4.
14. Lisher JP, Giedroc DP. 2013. Manganese acquisition and homeostasis at the host-pathogen interface. Front Cell Infect Microbiol 3:91. https://doi.org/10.3389/fcimb.2013.00091.
15. Eijkelkamp BA, McDevitt CA, Kitten T. 2015. Manganese uptake and streptococcal virulence. Biometals 28:491–508. https://doi.org/10.1007/s10534-015-9826-z.
16. Juttukonda LJ, Skaar EP. 2015. Manganese homeostasis and utilization in pathogenic bacteria. Mol Microbiol 97:216–228. https://doi.org/10.1111/mmi.13034.
17. Skaar EP. 2010. The battle for iron between bacterial pathogens and their vertebrate hosts. PLoS Pathog 6:e1000949. https://doi.org/10.1371/journal.ppat.1000949.
18. Gaca AO, Kajfasz JK, Miller JH, Liu K, Wang JD, Abranches J, Lemos JA. 2013. Basal levels of (p)ppGpp in Enterococcus faecalis: the magic beyond the stringent response. mBio 4:e00646-13. https://doi.org/10.1128/mBio.00646-13.
19. Vebø HC, Snipen L, Nes IF, Brede DA. 2009. The transcriptome of the nosocomial pathogen *Enterococcus faecalis* V583 reveals adaptive responses to growth in blood. PLoS One 4:e7660. https://doi.org/10.1371/journal.pone.0007660.
20. Vebø HC, Solheim M, Snipen L, Nes IF, Brede DA. 2010. Comparative genomic analysis of pathogenic and probiotic *Enterococcus faecalis* isolates, and their transcriptional responses to growth in human urine. PLoS One 5:e12489. https://doi.org/10.1371/journal.pone.0012489.
21. Arntzen MO, Karlskas IL, Skaugen M, Eijsink VG, Mathiesen G. 2015. Proteomic investigation of the response of *Enterococcus faecalis* V583 when cultivated in urine. PLoS One 10:e0126694. https://doi.org/10.1371/journal.pone.0126694.
22. Yan X, Zhao C, Budin-Verneuil A, Hartke A, Rincé A, Gilmore MS, Auffray Y, Pichereau V. 2009. The (p)ppGpp synthetase RelA contributes to stress adaptation and virulence in *Enterococcus faecalis* V583. Microbiology 155:3226–3237. https://doi.org/10.1099/mic.0.026146-0.
23. Vinella D, Albrecht C, Cashel M, D'Ari R. 2005. Iron limitation induces SpoT-dependent accumulation of ppGpp in *Escherichia coli*. Mol Microbiol 56:958–970. https://doi.org/10.1111/j.1365-2958.2005.04601.x.
24. Geiger T, Wolz C. 2014. Intersection of the stringent response and the CodY regulon in low GC Gram-positive bacteria. Int J Med Microbiol 304:150–155. https://doi.org/10.1016/j.ijmm.2013.11.013.
25. Kriel A, Brinsmade SR, Tse JL, Tehranchi AK, Bittner AN, Sonenshein AL, Wang JD. 2014. GTP dysregulation in *Bacillus subtilis* cells lacking (p)ppGpp results in phenotypic amino acid auxotrophy and failure to adapt to nutrient downshift and regulate biosynthesis genes. J Bacteriol 196:189–201. https://doi.org/10.1128/JB.00918-13.
26. Belitsky BR, Sonenshein AL. 2008. Genetic and biochemical analysis of CodY-binding sites in *Bacillus subtilis*. J Bacteriol 190:1224–1236. https://doi.org/10.1128/JB.01780-07.
27. Abrantes MC, Kok J, Lopes MDF. 2013. EfaR is a major regulator of *Enterococcus faecalis* manganese transporters and influences processes

involved in host colonization and infection. Infect Immun 81:935–944. https://doi.org/10.1128/IAI.06377-11.
28. Low YL, Jakubovics NS, Flatman JC, Jenkinson HF, Smith AW. 2003. Manganese-dependent regulation of the endocarditis-associated virulence factor EfaA of *Enterococcus faecalis*. J Med Microbiol 52:113–119. https://doi.org/10.1099/jmm.0.05039-0.
29. Muller C, Cacaci M, Sauvageot N, Sanguinetti M, Rattei T, Eder T, Giard JC, Kalinowski J, Hain T, Hartke A. 2015. The intraperitoneal transcriptome of the opportunistic pathogen *Enterococcus faecalis* in mice. PLoS One 10:e0126143. https://doi.org/10.1371/journal.pone.0126143.
30. Martin JE, Waters LS, Storz G, Imlay JA. 2015. The *Escherichia coli* small protein MntS and exporter MntP optimize the intracellular concentration of manganese. PLoS Genet 11:e1004977. https://doi.org/10.1371/journal.pgen.1004977.
31. Pugh SY, Knowles CJ. 1982. Growth of *Streptococcus faecalis* var. zymogenes on glycerol: the effect of aerobic and anaerobic growth in the presence and absence of haematin on enzyme synthesis. J Gen Microbiol 128:1009–1017.
32. Huycke MM, Moore D, Joyce W, Wise P, Shepard L, Kotake Y, Gilmore MS. 2001. Extracellular superoxide production by *Enterococcus faecalis* requires demethylmenaquinone and is attenuated by functional terminal quinol oxidases. Mol Microbiol 42:729–740. https://doi.org/10.1046/j.1365-2958.2001.02638.x.
33. Cross JH, Bradbury RS, Fulford AJ, Jallow AT, Wegmuller R, Prentice AM, Cerami C. 2015. Oral iron acutely elevates bacterial growth in human serum. Sci Rep 5:16670. https://doi.org/10.1038/srep16670.
34. Parkkinen J, von Bonsdorff L, Peltonen S, Gronhagen-Riska C, Rosenlof K. 2000. Catalytically active iron and bacterial growth in serum of haemodialysis patients after i.v. iron-saccharate administration. Nephrol Dial Transplant 15:1827–1834. https://doi.org/10.1093/ndt/15.11.1827.
35. Kehl-Fie TE, Zhang Y, Moore JL, Farrand AJ, Hood MI, Rathi S, Chazin WJ, Caprioli RM, Skaar EP. 2013. MntABC and MntH contribute to systemic *Staphylococcus aureus* infection by competing with calprotectin for nutrient manganese. Infect Immun 81:3395–3405. https://doi.org/10.1128/IAI.00420-13.
36. Damo SM, Kehl-Fie TE, Sugitani N, Holt ME, Rathi S, Murphy WJ, Zhang Y, Betz C, Hench L, Fritz G, Skaar EP, Chazin WJ. 2013. Molecular basis for manganese sequestration by calprotectin and roles in the innate immune response to invading bacterial pathogens. Proc Natl Acad Sci U S A 110:3841–3846. https://doi.org/10.1073/pnas.1220341110.
37. Kazmierczak KM, Wayne KJ, Rechtsteiner A, Winkler ME. 2009. Roles of rel_{Spn} in stringent response, global regulation and virulence of serotype 2 *Streptococcus pneumoniae* D39. Mol Microbiol 72:590–611. https://doi.org/10.1111/j.1365-2958.2009.06669.x.
38. Miethke M, Westers H, Blom EJ, Kuipers OP, Marahiel MA. 2006. Iron starvation triggers the stringent response and induces amino acid biosynthesis for bacillibactin production in *Bacillus subtilis*. J Bacteriol 188:8655–8657. https://doi.org/10.1128/JB.01049-06.
39. Hogg T, Mechold U, Malke H, Cashel M, Hilgenfeld R. 2004. Conformational antagonism between opposing active sites in a bifunctional RelA/SpoT homolog modulates (p)ppGpp metabolism during the stringent response [corrected]. Cell 117:57–68. https://doi.org/10.1016/S0092-8674(04)00260-0.
40. Gaca AO, Kudrin P, Colomer-Winter C, Beljantseva J, Liu K, Anderson B, Wang JD, Rejman D, Potrykus K, Cashel M, Hauryliuk V, Lemos JA. 2015. From (p)ppGpp to (pp)pGpp: characterization of regulatory effects of pGpp synthesized by the small alarmone synthetase of *Enterococcus faecalis*. J Bacteriol 197:2908–2919. https://doi.org/10.1128/JB.00324-15.
41. Sobota JM, Imlay JA. 2011. Iron enzyme ribulose-5-phosphate 3-epimerase in *Escherichia coli* is rapidly damaged by hydrogen peroxide but can be protected by manganese. Proc Natl Acad Sci U S A 108:5402–5407. https://doi.org/10.1073/pnas.1100410108.
42. Ogunniyi AD, Mahdi LK, Jennings MP, McEwan AG, McDevitt CA, Van der Hoek MB, Bagley CJ, Hoffmann P, Gould KA, Paton JC. 2010. Central role of manganese in regulation of stress responses, physiology, and metabolism in *Streptococcus pneumoniae*. J Bacteriol 192:4489–4497. https://doi.org/10.1128/JB.00064-10.
43. Caymaris S, Bootsma HJ, Martin B, Hermans PW, Prudhomme M, Claverys JP. 2010. The global nutritional regulator CodY is an essential protein in the human pathogen *Streptococcus pneumoniae*. Mol Microbiol 78:344–360. https://doi.org/10.1111/j.1365-2958.2010.07339.x.
44. Château A, van Schaik W, Six A, Aucher W, Fouet A. 2011. CodY regulation is required for full virulence and heme iron acquisition in *Bacillus anthracis*. FASEB J 25:4445–4456. https://doi.org/10.1096/fj.11-188912.
45. Wexselblatt E, Oppenheimer-Shaanan Y, Kaspy I, London N, Schueler-Furman O, Yavin E, Glaser G, Katzhendler J, Ben-Yehuda S. 2012. Relacin, a novel antibacterial agent targeting the stringent response. PLoS Pathog 8:e1002925. https://doi.org/10.1371/journal.ppat.1002925.
46. Andresen L, Varik V, Tozawa Y, Jimmy S, Lindberg S, Tenson T, Hauryliuk V. 2016. Auxotrophy-based high throughput screening assay for the identification of *Bacillus subtilis* stringent response inhibitors. Sci Rep 6:35824. https://doi.org/10.1038/srep35824.
47. Kristich CJ, Chandler JR, Dunny GM. 2007. Development of a host-genotype-independent counterselectable marker and a high-frequency conjugative delivery system and their use in genetic analysis of *Enterococcus faecalis*. Plasmid 57:131–144. https://doi.org/10.1016/j.plasmid.2006.08.003.
48. Leenhouts K, Buist G, Bolhuis A, ten Berge A, Kiel J, Mierau I, Dabrowska M, Venema G, Kok J. 1996. A general system for generating unlabelled gene replacements in bacterial chromosomes. Mol Gen Genet 253:217–224. https://doi.org/10.1007/s004380050315.
49. Kristich CJ, Wells CL, Dunny GM. 2007. A eukaryotic-type Ser/Thr kinase in *Enterococcus faecalis* mediates antimicrobial resistance and intestinal persistence. Proc Natl Acad Sci U S A 104:3508–3513. https://doi.org/10.1073/pnas.0608742104.
50. Terleckyj B, Willett NP, Shockman GD. 1975. Growth of several cariogenic strains of oral streptococci in a chemically defined medium. Infect Immun 11:649–655.
51. Abranches J, Chen YY, Burne RA. 2004. Galactose metabolism by *Streptococcus mutans*. Appl Environ Microbiol 70:6047–6052. https://doi.org/10.1128/AEM.70.10.6047-6052.2004.
52. Nguyen PT, Abranches J, Phan TN, Marquis RE. 2002. Repressed respiration of oral streptococci grown in biofilms. Curr Microbiol 44:262–266. https://doi.org/10.1007/s00284-001-0001-0.